

Ultrastructural Mechanical and Material Characterization of Fossilized Bone

Sara E. Olesiak¹, Michelle Oyen², Matthew Sponheimer³, Jaelyn J. Eberle⁴, and Virginia L. Ferguson¹

¹Department of Mechanical Engineering, University of Colorado, Boulder, CO, 80309

²Engineering, Cambridge University, Cambridge, CB2 1PZ, United Kingdom

³Department of Anthropology, University of Colorado, Boulder, CO, 80309

⁴Department of Geological Sciences and University of Colorado Museum, University of Colorado, Boulder, CO, 80309

ABSTRACT

Bone plays a key role in the paleontological and archeological records and can provide insight into the biology, ecology and the environment of ancient vertebrates. Examination of bone at the tissue level reveals a definitive relationship between nanomechanical properties and the local organic content, mineral content, and microstructural organization. However, it is unclear as to how these properties change following fossilization, or diagenesis, where the organic phase is rapidly removed and the remaining mineral phase is reinforced by the deposition of apatites, calcites, and other minerals. While the process of diagenesis is poorly understood, its outcome clearly results in the potential for dramatic alteration of the mechanical response of biological tissues. In this study, fossilized specimens of mammalian long bones, collected from Colorado and Wyoming, were studied for mechanical variations. Nanoindentation performed in both longitudinal and transverse directions revealed preservation of bone's natural anisotropy as transverse modulus values were consistently smaller than longitudinal values. Additionally, modulus values of fossilized bone from 35.0 to 89.1 GPa increased linearly with logarithm of the sample's age. Future studies will aim to clarify what mechanical and material elements of bone are retained during diagenesis as bone becomes part of the geologic milieu.

INTRODUCTION

Bone is a living tissue that serves roles ranging from physiological to structural. Over time, cell-mediated remodeling replaces immature woven bone with lamellar bone that is more highly organized and mineralized. Studies of chemical signals and histology from ancient bone and teeth have been used to investigate paleodiets, migration, age, and paleoclimates [1-6]. Bone is a living tissue which undergoes growth and remodeling throughout its life and, post-mortem, is altered to varying degrees through fossilization or diagenetic processes.

An understanding of diagenetic post-mortem change is needed to interpret the data extracted from paleontological and archeological bone. Alterations occur at length scales ranging from the nanoscale to the macroscopic scale. Partial or complete dissolution, recrystallization, uptake of trace elements, erosion, and changes in porosity can cause significant changes in material structure and composition. These diagenetic changes have been well documented [7-

14], yet no comprehensive models of the effects of diagenesis on bone structure and composition have been proposed. Nielsen-March and Hedges investigated the correlation of the basic diagenetic parameters: histology, protein content, porosity, crystallinity and carbonate content from a large set of European sites [14]. They characterized the diagenetic properties of bones in different burial environments; however, these trends represent generalized diagenetic change and do not characterize detailed structural and chemical changes. A complete, multi-scale analysis of bone material and chemical post-mortem alterations is needed to fully understand diagenesis.

Over the last ten years nanoindentation has become a popular tool to investigate the nanomechanical properties of mineralized tissues and individual structural features. The mechanical properties of mineralized tissues are determined by compositional and microstructural properties. This study is the first to use nanoindentation to provide insight into the ultra-structure and compositional properties of fossilized bone, and should ultimately provide insight into the complex process of diagenesis.

EXPERIMENTAL METHODS

Three fossilized mammalian long bones from various ages were investigated for compositional and mechanical variations. Specimens were collected by University of Colorado Museum (UCM) parties in Wyoming and Colorado (detailed locality information is on file at the UCM.): UCM Specimen No. 100371 is Pleistocene in age (or approximately 1 Million years ago (Ma)), UCM Specimen No. 100373 from the Miocene epoch (~ 15 Ma), UCM Specimen No. 100372 from Bridger C (~ 50 Ma). Sample ages were approximated using mammalian biostratigraphy or the North American Land Mammal Ages (or NALMA). Samples will be referred to by approximate age.

Each sample was embedded in polymethylmethacrylate (PMMA) under vacuum and sectioned transversely to the long axis of the bone using a diamond wafering saw (Isomet: Buehler, Lake Bluff, IL). Embedding in PMMA stabilized the delicate fossilized material and allowed for sample preparation; additionally, the low modulus value of PMMA was likely to contribute minimally to the measured mechanical properties of the samples. The transverse axis runs parallel to most Haversian canals whereas the longitudinal axis is perpendicular to the Haversian canal, along the long axis of the bone. Transverse and longitudinal surfaces were prepared for testing on individual slices of each fossil by sectioning each sample based on gross morphology. Orientation was confirmed with microscopical analysis of structural features. Each surface was ground with 320, 600 and then 1200 grit silicon carbide paper. The surfaces were then polished on a microcloth with progressively finer diamond suspension paste to a 0.25 μm finish.

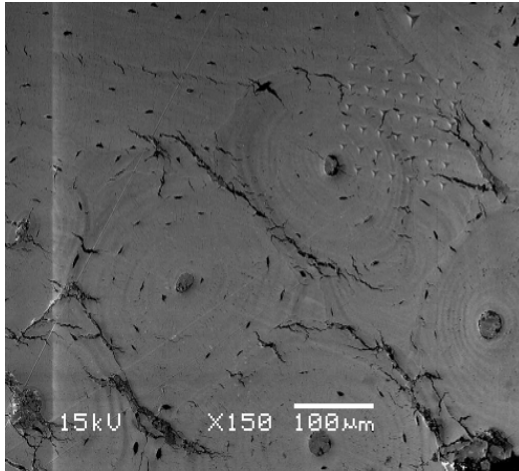


Figure 1: Longitudinal axis 6X6 indent array over osteonal and interstitial bone, 15 Ma sample

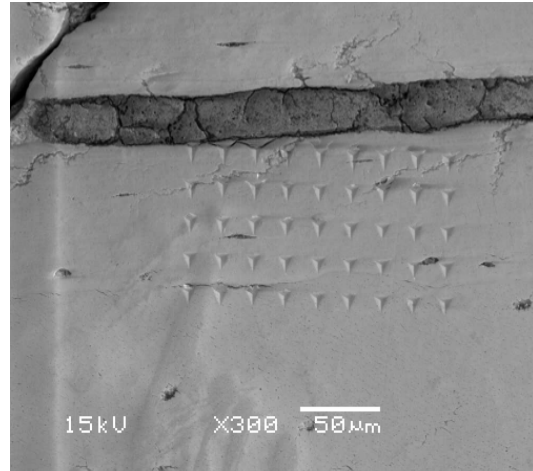


Figure 2: Transverse axis 4X9 indent array starting at Haversian canal, 15 Ma sample

Depth-control nanoindentation tests (NANO IndenterXP, MTS Systems Co., Oak Ridge, TN) were performed on the embedded bone samples. Bones were loaded with a Berkovich tip to 1500 nm max depth. Indentation arrays were placed in both the transverse and longitudinal directions. Longitudinally, two indent arrays of at least 6X6 indents were placed with the first indent in the Haversian canal. The square array, with 20µm spacing, covered both osteonal and interstitial bone (Fig. 1). For transverse sections 4X9 indent arrays with 20 µm spacing were located along the Haversian canal and propagated outward (Fig. 2). Additionally, the sample aged 15 Ma contained trabecular bone in which a 6X6 indent array with 20µm spacing was placed. Measurements from sites close to cracks, flaws, edges or other voids were not used. In this study, the Poisson's ratio was assumed to be the same as for modern bone, $\nu=0.3$. The unloading data were used along with the Oliver-Pharr method to determine the modulus and hardness of each sample [15].

Quantitative back-scattered electron (qBSEM) imaging was performed on the 15 Ma sample in both the longitudinal and transverse directions (qBSEM; 15kV, 13mm working distance). Compositional information was acquired with energy dispersive analysis with x-rays (EDAX) on four indents, one placed on each edge of the array, of both the transverse and longitudinal indent arrays.

RESULTS AND DISCUSSION

Modulus values of fossilized cortical bone tested in the transverse direction were 9-59% lower than values measured in the longitudinal direction (Table 1, Fig. 3). Modern bone had a 25% decrease from longitudinal to transverse modulus values [16] (Table 1). A consistently smaller transverse modulus value in fossilized bone reflects anisotropy seen in modern bone samples and signifies some structural and mechanical preservation. The longitudinal data were divided into osteonal and interstitial indentation sites (Table 2). Interstitial bone had larger modulus values for all samples except the 1 Ma sample. This is consistent with modern bone which has a 13% larger modulus value for interstitial than osteonal bone [17]. Backscattering scanning electron microscopy has demonstrated that interstitial bone is more mineralized than

osteonal bone [18]. Additionally, osteonal bone is younger and therefore less mineralized than interstitial bone, which may result in reduced Young's moduli. Trabecular bone was found only on the 15 Ma sample, and the modulus value was similar to cortical values.

Table 1. Values of E (SD) determined by nanoindentation in cortical (longitudinal and transverse directions) and trabecular bone. E' values of horse bone embedded in PMMA [16]

	E /GPa Longitudinal	E /GPa Transverse	E /GPa Trabecular
1 Ma	34.53 (4.30)	14.01 (2.45)	
15 Ma	72.89 (8.67)	66.15 (2.88)	75.09 (4.94)
50 Ma	89.07 (5.33)	76.25 (3.55)	
Modern horse bone	25.8 (2.1)	19.4 (2.1)	

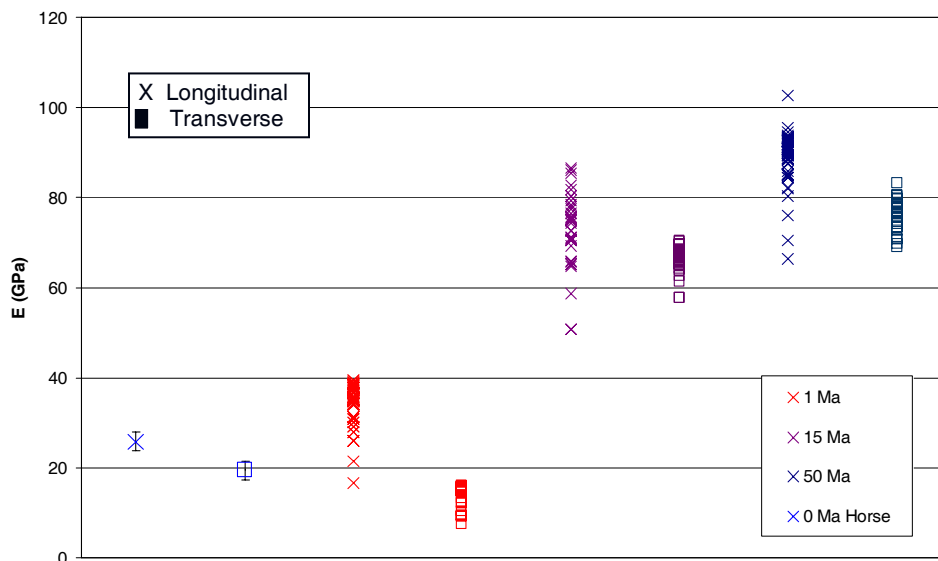


Figure 3: Cortical bone indents: Longitudinal vs. Transverse. Ma = million years ago. E' values of horse bone embedded in PMMA, error bars = SD [16].

Table 2. Values of E (STD) of cortical bone divided into primary osteonal and interstitial bone. Ma= million years ago. Dried human tibia embedded in epoxy [17]

	E /GPa Osteonal	E /GPa Interstitial
1 Ma	34.56 (4.10)	34.50 (4.50)
15 Ma	69.84 (10.84)	75.03 (6.62)
50 Ma	86.85 (7.34)	90.53 (2.67)
Modern Human Tibia	22.4 (1.3)	25.8 (0.7)

Large amounts of scatter were apparent in the measured modulus values of preserved bone. Fossilized samples on average covered a 30 GPa range of modulus values. The coefficient of variation ($COV = (\text{standard deviation}/\text{mean}) * 100$), provides a measure of the scatter in modulus values. In general the COV was greater in osteonal than in interstitial bone (Fig. 4). This trend was also seen in modern bone, and might be related to the high variability in ultrastructural orientation in a single osteon. Additionally, COV was generally larger in fossilized bone than in modern bone (Fig. 4). The large and diverse changes caused by diagenesis may help to explain the high variability of fossilized bone. Modulus values of all types of bone increased linearly with logarithm of the age of each sample (Fig. 5). This is consistent with the idea that fossils continue to mineralize through time. An increase in mineral is directly related to an increase in stiffness; this follows composites theory where small increases in mineral content can result in large increases in modulus.

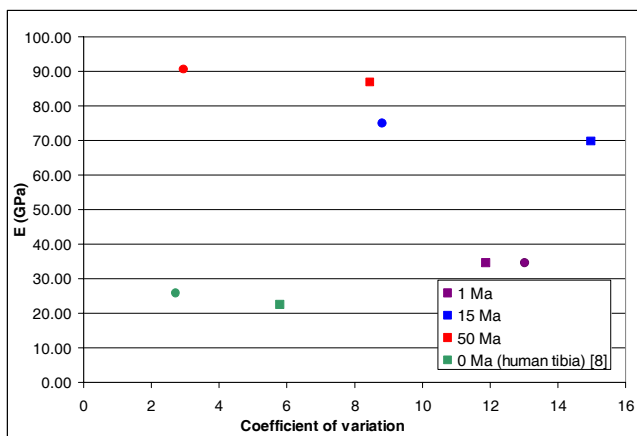


Figure 4: Percent coefficient of variation of osteonal = ■ and interstitial = ● bone.

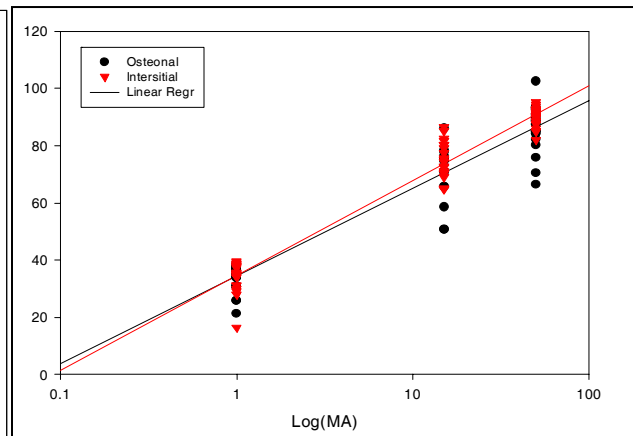


Figure 5: Modulus variation with the log of time.

Contaminate analysis revealed C, O, P, Ca at all indents sites and F, Mg, Al, Si, Na, Cs, and Y at various indents sites on the 15 Ma sample. This initial analysis reveals the likely presence of calcium phosphate with other trace elements, which confirms expected results. Some variability was seen within indent arrays, whereas large changes were seen in trace element composition across indent arrays. This variability in composition is a result of diagenetic processes and may contribute to the variability of measured mechanical properties. Current data demonstrate expected compositions and future advances in this area hope to reveal potential influences of mineral composition on material properties.

CONCLUSIONS

The mechanical properties of preserved bone were highly altered from modern bone. However, the consistently lower transverse modulus values, as compared to longitudinal, reflect the preservations of the anisotropy of modern bone. Structural and compositional variations introduced by diagenesis contribute to the highly variable mechanical properties found in individual samples of aged bone. Over time the increase of Young's modulus parallels the infilling of mineral at high concentrations as seen in modern bone. Nanoindentation of fossilized

bone displays key trends which reflect the original structure and may provide insight into complex diagenetic processes.

ACKNOWLEDGMENTS

Thank you to the University of Colorado museum for access to samples. This work was funded through the NSF Graduate Research Fellowship.

REFERENCES

1. Yang Wang and Thure E. Cerling, *Palaeogeography, Palaeoclimatology, Palaeoecology* **107** (3-4), 281 (1994).
2. David Lubell, Mary Jackes, Henry Schwarcz et al., *Journal of Archaeological Science* **21** (2), 201 (1994).
3. Brian M. Butler, Douglas B. Hanson, Rosalind L. Hunter-Anderson, Harold W. Krueger and Stanley H. Ambrose, *American Journal of Physical Anthropology* **104** (3), 343 (1997).
4. Antoine Zazzo, Andre Mariotti, Christophe Lecuyer et al., *Palaeogeography, Palaeoclimatology, Palaeoecology* **186** (1-2), 145 (2002).
5. T. D. Price, J. H. Burton, and R. A. Bentley, *Archaeometry* **44**, 117 (2002).
6. Thure E. Cerling and Zachary D. Sharp, *Palaeogeography, Palaeoclimatology, Palaeoecology* **126** (1-2), 173 (1996).
7. R. E. M. Hedges and A. R. Millard, *Journal of Archaeological Science* **22** (2), 155 (1995).
8. I. Reiche, L. Favre-Quattropani, C. Vignaud et al., *Measurement Sci. & Tech.* **14** (9), 1608 (2003).
9. E. Badone and R. M. Farquhar, *Journal of Radioanalytical Chemistry* **69** (1-2), 291 (1982).
10. T. A. Elliott and G. W. Grime, *Nuclear Inst. and Methods in Physics Research Section B: Beam Interactions with Mater. and Atoms* **77** (1-4), 537 (1993).
11. Matthew J. Kohn, Margaret J. Schoeninger, and William W. Barker, *Geochimica et Cosmochimica Acta* **63** (18), 2737 (1999).
12. L. Quattropani, L. Charlet, H. de Lumley et al., *Mineralogical Mag.* **63** (6), 801 (1999).
13. C. N. G. Trueman, A. K. Behrensmeyer, N. Tuross et al., *Journal of Archaeological Science* **31** (6), 721 (2004).
14. Christina M. Nielsen-Marsh and Robert E. M. Hedges, **27** (12), 1139 (2000).
15. W. C. Oliver and G. M. Pharr, *J. of Mater. Research* **7** (6), 1564 (1992).
16. Vanessa Koonjul, Amanpreet K. Bembey, Andrew J. Bushby, Virginia L. Ferguson and Alan Boyde, *Mater. Res. Soc. Symp. Proc.* **841**, R2.8.1 (2005).
17. J. Y. Rho, T. Y. Tsui, and G. M. Pharr, *Biomaterials* **18** (20), 1325 (1997).
18. J.M. Dorlot, G. L'Esperance, and A. Meunier, *Trans. 32nd Orthop. Res. Soc.* **11**, 330 (1986).